Non-linear Trajectory Optimization Techniques for Interconnection Compliance Applications

Rodrigo Henriquez-Auba & Jose Daniel Lara
National Renewable Energy Laboratory, Golden, CO
{rodrigo.henriquezauba, josedaniel.lara}@nrel.gov

***Abstract*—This paper introduces a framework that employs an optimization-based approach via trajectory optimization to parametrize machine and inverter models in compliance with interconnection requirements. The approach leverages direct collocation techniques to implement continuous-time dynamics in a non-convex optimization problem that simultaneously optimizes selected parameters over an approximation of the post-perturbation trajectory. We present two example cases, one for tuning a synchronous generator Automatic Voltage Regulator (AVR) gain and one for tuning the outer control of a Grid-Forming (GFM) inverter. The results include time domain simulations for perturbations outside of the sample used to optimize the parameters that showcase the performance of the components to the required constraints.**

***Index Terms*—Parameter Tuning, Trajectory Optimization, Inverter-Based Resources, Simulation**

I. Introduction

The increasing integration of multiple devices through power electronics is reshaping the dynamic performance of power systems. As new controllers interact with the grid, these interactions are anticipated to introduce dynamics that affect overall system stability [1]. With the rapid incorporation of large-scale loads, such as data centers, into the grid, it is becoming increasingly important for operators and manufacturers to expedite the compliance testing and parameter tuning phases of the interconnection process [2]. Ensuring that new devices meet interconnection requirements, such as the IEEE 2800 standard, is critical to maintaining grid reliability. This process requires careful parametrization of the various controllers.

Although many devices help regulate voltage and frequency, synchronous generators and inverter-based resources remain essential to manage these signals across different buses [3], [4]. Proper parameter tuning is vital to ensure that new resources comply with interconnection requirements, including IEEE 2800, NERC reliability standards, and regional grid codes, which define specific operating limits for voltage regulation, frequency response, and fault-riding capabilities. These standards mandate that resources remain connected during defined voltage excursions and frequency deviations, while providing dynamic reactive support during disturbances. Analyses are conducted to confirm that resources can meet steady-state voltage regulation requirements (typically ±0.95 to 1.05 per unit) and maintain transient stability following contingencies. However, default control settings often do not satisfy these standards, particularly as sources incorporate increasing limiters and discrete control behaviors.

Control engineers have developed various parameter tuning approaches based on the control structure. For PID controllers, the primary goal of tuning is to eliminate dominant poles, effectively canceling out oscillatory modes to optimize system response. PID controllers have established handbooks with tuning rules that are based on step responses, specific decay rates, defined closed-loop responses, and methods such as Ziegler-Nichols [5], [6]. Methods like modulus optimum, symmetrical optimum, and pole placement have been widely used for tuning voltage source converter (VSC) applications, including high-voltage direct current (HVDC) applications [7].

Generally, plants are nonlinear with discrete processes, and parameter tuning requires engineering expertise and manual adjustments, making it challenging to automate. Achieving effective parameter values that produce the desired response across multiple operating conditions typically involves significant trial and error. One step toward automation is the use of *trajectory optimization*. In simple terms, trajectory optimization refers to a set of methods aimed at determining the optimal trajectory by selecting inputs, or parameters, to the system—known as controls—over time [8].

Trajectory optimization combines the continuous nonlinear dynamics of plants and controllers with optimization techniques, typically by embedding their (discretized) dynamics into a nonlinear mathematical program. In this paper, we use *direct collocation methods* that result in a non-convex optimization problem on which dynamic states and selected parameters are variables to optimize. The proposed framework has been implemented in the open-source package `PowerTrajectoryOpt.jl`[1] including the case study for reproducibility. The contributions of the paper are as follows:

- A two-stage trajectory optimization approach to optimize parameters applicable for Quasi-Static Phasor (QSP) and Electromagnetic Transients Models (EMT) over a set of perturbations.
- Implementation of the trajectory approach as a two step procedure including the optimization and verification applied to an AVR model and virtual synchronous machine grid-forming inverter model.
- The implementation of the proposed model and process in an open-source package for power system analysis.

This research was supported by the U.S. Department of Energy under contract AC36-08GO2830.

[1] https://github.com/NREL-Sienna/PowerTrajectoryOpt.jl

979-8-3315-8138-1

II. Trajectory Optimization Implementation

In this section, we will review the implementation for trajectory optimization based on direct collocation. Consider a power system dynamic model represented with differential-algebraic equations:

$$\frac{d\boldsymbol{x}(t)}{dt} = \boldsymbol{f}(\boldsymbol{x}(t), \boldsymbol{y}(t), \boldsymbol{\eta}), \quad \boldsymbol{x}(t_0) = \boldsymbol{x}^0, \tag{1a}$$

$$\frac{d\boldsymbol{y}(t)}{dt} = \boldsymbol{g}(\boldsymbol{x}(t), \boldsymbol{y}(t), \boldsymbol{\psi}), \quad \boldsymbol{y}(t_0) = \boldsymbol{y}^0, \tag{1b}$$

where $\boldsymbol{x}$ are the states for the injectors, and $\boldsymbol{y}$ are the network circuit states, and $\boldsymbol{\eta}, \boldsymbol{\psi}$ are the model parameters. In QSP models, typically $d\boldsymbol{y}(t)/dt = 0$ to make the network equations algebraic and modeled via the admittance matrix relationship between device current injections and bus voltages.

The direct collocation method transcribes the continuous-time trajectory into an optimization problem. Given the stiff nature of power system dynamics, a trapezoidal collocation (via the trapezoidal rule) is used to discretize the equations. Consider a N-steps time discretization $k = 0, 1, \ldots, N-1$, the dynamics can be approximated as:

$$\boldsymbol{x}_{k+1} - \boldsymbol{x}_k = \frac{h_k}{2}\left(\boldsymbol{f}_{k+1} + \boldsymbol{f}_k\right), \quad k = 0, \ldots, N-2 \tag{2a}$$

$$\boldsymbol{y}_{k+1} - \boldsymbol{y}_k = \frac{h_k}{2}\left(\boldsymbol{g}_{k+1} + \boldsymbol{g}_k\right), \quad k = 0, \ldots, N-2, \tag{2b}$$

where $\boldsymbol{x}_k$, $\boldsymbol{y}_k$ are the decision variables with $\boldsymbol{f}_k \equiv \boldsymbol{f}(\boldsymbol{x}_k, \boldsymbol{y}_k, \boldsymbol{\eta})$ and $\boldsymbol{g}_k \equiv \boldsymbol{g}(\boldsymbol{x}_k, \boldsymbol{y}_k, \boldsymbol{\psi})$. In this paper, we use a uniform step size $h_k \equiv t_{k+1} - t_k = h$, selected for the specific problem studied (e.g. QSP or EMT). In the case of QSP modeling, equation (2b) turns into the constraints $g_k = 0$ due to the elimination of the differential terms in (1b).

A. Non-convex mathematical program

The parameter tuning approach involves selecting a subset of parameters $\boldsymbol{p} \subset \boldsymbol{\eta} \cup \boldsymbol{\psi}$ that are of interest to optimize. It is required to define a specific objective function J depending on the control objectives. For instance, minimizing losses, tracking a desired trajectory, or achieving minor deviations to selected setpoints. Furthermore, we include additional constraints $\boldsymbol{r}$ to represent performance requirements, such as the maximum voltage dip and ride-through behavior. Finally, the mathematical program can be posed as follows:

$$\min_{\boldsymbol{x},\boldsymbol{y},\boldsymbol{p}} \quad \sum_{k=0}^{N-1} J_k(\boldsymbol{x}, \boldsymbol{y}, \boldsymbol{p}) \tag{3a}$$

$$\text{s.t.} \quad \boldsymbol{x}_0 = \boldsymbol{x}^0, \ \boldsymbol{y}_0 = \boldsymbol{y}^0, \tag{3b}$$

$$\text{(2a)–(2b)} \tag{3c}$$

$$\boldsymbol{r}_k = 0, \qquad k = 0, \ldots, N-1 \tag{3d}$$

In the application of trajectory optimization of generation compliance introduces a non-linear problem with the addition of $P(t) = \mathcal{R}(v(t)i(t))$ and $Q(t) = \mathcal{I}(v(t)i(t))$ which is implement as part of the f_k functions. However, given that there are known limits to the voltages and currents, appropriate bounds can be calculated for the variables and their products to facilitate convergence [9].

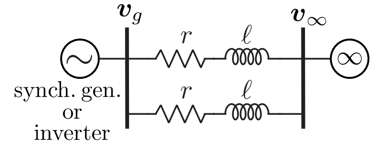

Fig. 1. Device against infinite bus.

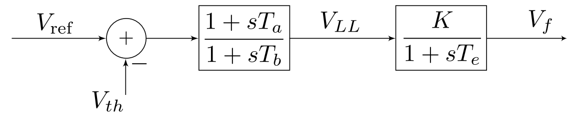

Fig. 2. Simplified excitation system model.

B. Solver Initialization

The resulting optimization model is highly non-convex, and without careful initialization of the variables for the solver, it is likely that no solution will be found when optimizing parameters. I.e, a flat initialization with zeros over the trajectory as well as the initial conditions will result in a failed solve. In our proposed approach, the problem must be initialized in a steady-state condition ($\boldsymbol{f}_0 = 0$), and then perturbed to enforce a change in the states. The steady-state solution for the variables $\boldsymbol{x}_0, \boldsymbol{y}_0$ is a good warm start for the variables at every time step k.

Particular attention must be paid to the question whether the parameters that are being optimized affect the steady-state solution of the variables. In such cases, the terms $\boldsymbol{x}^0, \boldsymbol{y}^0$ depend on the parameters to be optimized and must be explicitly included in constraints (3b). An example of this scenario for AVR tuning is presented in the next section. In these cases, the warm start for the solver can be included by selecting an initial guess for the parameters to be optimized. We obtain the initial conditions for the trajectory problem by initializing the pre-perturbation system using `PowerSimulationsDynamics.jl` (PSID) [10].

III. Study Cases and Discussion

This section demonstrates how the trajectory optimization approach is applied to optimize the parameters of a synchronous machine AVR controller and a grid-forming outer control, specifically a virtual synchronous machine outer controller. The study cases utilize one device (machine or inverter) connected via a double-circuit line to an infinite bus (see Fig. 1), focusing on optimizing specific key parameters. The optimized parameters through trajectory optimization are then updated in a dynamic simulation using (PSID) to validate the performance across the perturbations. The models and parameters used are available in the scripts folder in the `PowerTrajectoryOpt.jl` repository. In this paper, the open-source solver `Ipopt` is used to solve the optimization problems and the HSL solver [11].

A. Simplified Excitation System (SEXS) model

The Simplified Excitation System (SEXS) AVR model presented in Fig. 2 is a simple AVR that consists of a lead-

979-8-3315-8138-1

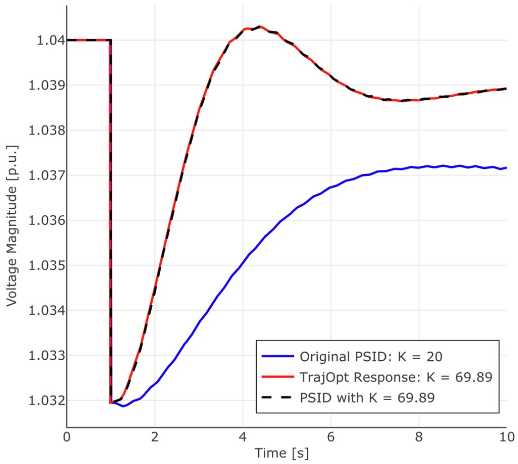

Fig. 3. AVR response against a circuit trip.

lag block with an exciter and regulator that controls the field voltage based on the magnitude of the measured voltage. The AVR dynamics are described with:

$$\frac{dV_f}{dt} = \frac{1}{T_e}(K \cdot V_{LL} - V_f) \tag{4a}$$

$$\frac{dV_r}{dt} = \frac{1}{T_b}\left[\left(1 - \frac{T_a}{T_b}\right) - V_r\right] \tag{4b}$$

$$\text{with } V_{LL} = V_r + \frac{T_a}{T_b}(V_{\text{ref}} - V_{th}) \tag{4c}$$

where V_{th} is the measured voltage magnitude of the bus where the generator is connected. The AVR is connected to the 4-state synchronous generator model commonly known as the one-d one-q axis model, described in Chapter 15.1.6 in [12].

1) Initialization setup: We are interested in optimizing the AVR gain K while initializing the variables in steady state from a power flow solution. For that, it is necessary to solve V_{ref} such that the terminal voltage of the generator matches the voltage magnitude imposed in the power flow case. For this AVR model, for a given terminal voltage V_{th0}, the field voltage V_{f0} does not depend on K, but V_{ref} and V_{r0} will impose the following constraints:

$$V_{\text{ref}} = \frac{K \cdot V_{th0} + V_{f0}}{K} \tag{5a}$$

$$V_{r0} = \frac{V_{f0}(T_b - T_a)}{K \cdot T_b} \tag{5b}$$

2) Single circuit trip: We aim to optimize the gain K so that the voltage recovers more quickly after a circuit trip. For that, we propose the following objective function:

$$J = \sum_{k=0}^{N-1} \left(V_{th,k} - V_{th}^0\right)^2 \tag{6}$$

imposing the circuit trip occurring at $t = 1$s. We use a fixed time-step discretization of 10 ms, and impose a bound for $K \in [0, 100]$. The optimization problem yields a solution of $K = 69.89$, as depicted in Fig. 3, resulting in a faster response without significant overshoot. Additionally, the gain is validated using PSID, yielding the same response showcasing he validity of the approach.

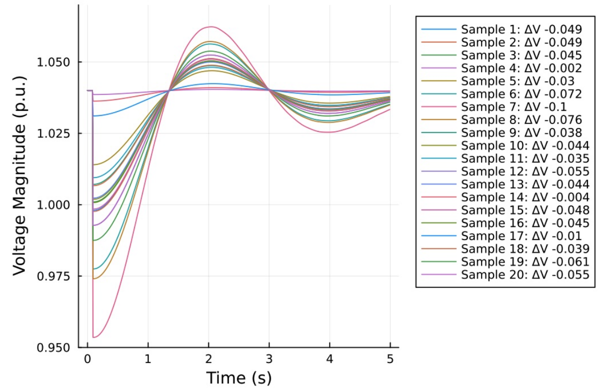

Fig. 4. Response against multiple voltage dips. $K^* = 300$ (max).

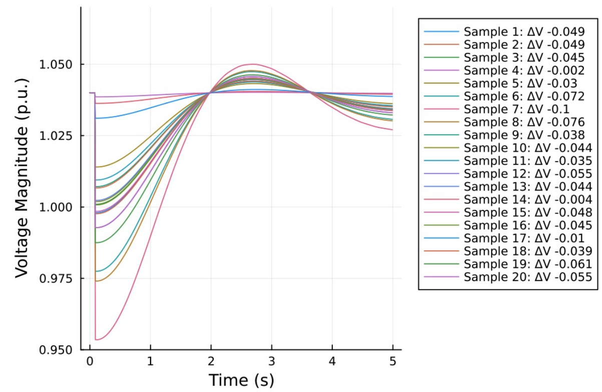

Fig. 5. Response with bounded voltage constraints. $K^* = 177.42$.

3) Simultaneous voltage dips: One of the benefits about trajectory optimization is that it is possible to pose multiple disturbances in a single optimization trajectory, such that the parameter is optimized to respond against a subset of all the disturbances. Fig. 4 shows the optimized response against 20 voltage dips independent scenarios that occur on the infinite bus. The solution finds $K = 300$ (maximum allowed value), but such a response in some scenarios has an overshoot greater than 1.05 p.u., which lies outside the permited operational range. Imposing a constraint on the terminal voltage to not exceed 1.05 p.u, results in $K = 177.42$, with trajectories depicted in Fig. 5. It can be observed that the response is indeed slower, but with a smaller overshoot, satisfying the performance requirement of $V_{th,k} \leq 1.05$ at every time step and for every scenario.

B. Virtual Synchronous Machine Damping

One of the most common grid-forming inverter control techniques is using a virtual synchronous machine (VSM) approach to emulate a synchronous generator. One key benefit of grid-forming inverters is that they can synchronize with the grid without requiring a phase-locked loop (PLL) [13]. However, if a PLL is available for estimating the grid fre-

979-8-3315-8138-1

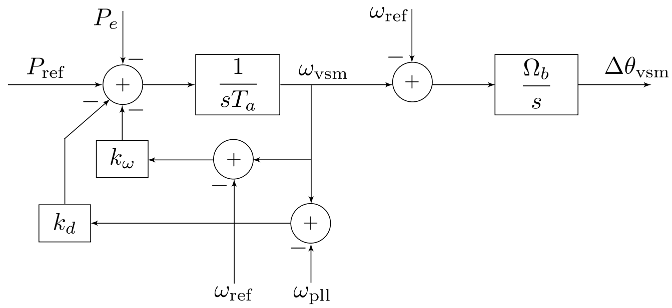

Fig. 6. Virtual Synchronous Machine outer control with additional PLL frequency damping.

quency, it can be used for an additional damping term in the VSM control. Fig. 6 shows a typical VSM outer control block diagram with an additional damping term $k_d(\omega_{\text{vsm}} - \omega_{\text{pll}})$.

The inverter is a $dq0$-EMT 17-state model with a 2-state VSM outer control model, a 1-state V/q reactive power droop model, a 4-state inner voltage and current control, a 6-state LCL filter and a 4-state PLL model. The dynamic grid-forming model is described in detail in our previous work [14]. For space considerations, we refer the reader to that reference for the differential equations model, and we focus on the VSM outer control dynamics:

$$\frac{d\Delta\theta_{\text{vsm}}}{dt} = \Omega_b(\omega_{\text{vsm}} - \omega_{\text{sys}}) \tag{7a}$$

$$\frac{d\omega_{\text{vsm}}}{dt} = \frac{1}{T_a}\left(P_{\text{ref}} - P_e - k_\omega(\omega_{\text{vsm}} - \omega_{\text{sys}}) - k_d(\omega_{\text{vsm}} - \omega_{\text{pll}})\right) \tag{7b}$$

where ω_{sys} is the system frequency given by the infinite bus ($\omega_{\text{sys}} = 1.0$ p.u.), ω_{pll} is the grid frequency estimated by the PLL, P_e is the electric power measured at the inverter filter, and Ω_b is the nominal frequency at $2\pi 60$ rad/s. For this case study, we are looking to optimize the new damping parameter k_d. We note that in steady-state $\omega_{\text{pll}} = \omega_{\text{vsm}} = \omega_{\text{sys}} = 1.0$, so optimizing k_d has no effect in the initial conditions setup.

1) Desired Power Trajectory: Relevant performance for grid-forming inverters is their capability to quickly increase their power output by updating it's power reference P_{ref}. Trajectory optimization allows us to give a smooth desired power command trajectory, optimizing $k_d \in [0, 2000]$ to follow as closely as possible to the provided command. The following objective function is used to achieve that:

$$J = \sum_{k=0}^{N-1} \left(P_{e,k} - P_k^{\text{command}}\right)^2 \tag{8}$$

Fig. 7 shows the active power response after a change in P_{ref} at $t = 1$ s from 50 to 69.5 MW. We observe that without the additional damping term, the default parameters for the inverter result in significant overshoot. By optimizing the new damping term k_d, a significant overdamped response is obtained, closer to the desired smooth trajectory.

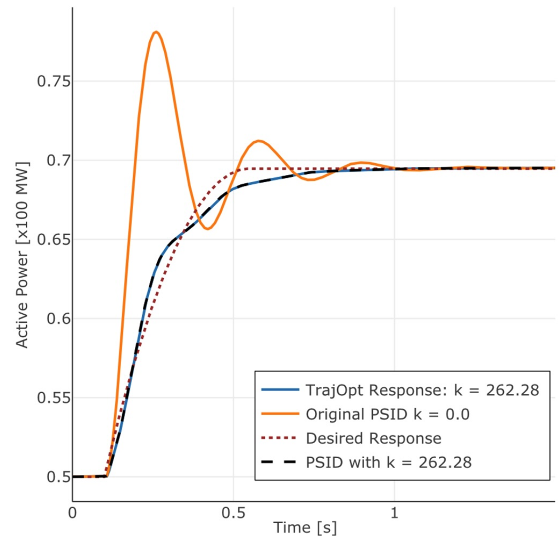

Fig. 7. Active power response for a P_{ref} step change.

The solution obtained is $k_d = 262.28$, with a clock time of 12.94 s, using a fixed discretization with a time-step resolution of 1 ms.

2) Simultaneous voltage dips: We tested against 20 perturbations of voltage dips at the infinite bus, but in this case we optimized k_d to recover the active power to 50 MW. For that purpose, the following objective function is used:

$$J = \sum_{k=0}^{N-1} \left(P_{e,k} - P_{e,0}\right)^2 \tag{9}$$

with $P_{e,0} = 50$ MW. Fig. 8 shows the active power response against the changes in voltage magnitude at infinite bus for the optimal $k_d = 93.23$. For comparison, Fig. 9 depicts the response without damping k_d, while Fig. 10 presents the response using the maximum k_d available at $k_d = 2000$.

Without k_d damping, the response has overshoot and takes additional time to return to the original dispatch at 50 MW. In contrast, with excessive damping at $k_d = 2000$, the response is overdamped, but takes around 5 seconds to get the active power back to 50 MW. Our proposed trajectory optimization approach is able to find the balance of an overdamped response but with a significantly faster recovery to the 50 MW dispatch.

C. Implementation details

It is crucial to remember that trajectory optimization for compliance applications will pose a non-convex optimization problem, so no guaranties can be provided for an optimal global solution. However, as this paper shows, significant improvements can be achieved if certain aspects are properly considered:

- Variables must be initialized correctly. Good performance is observed if the variables are warm started in the initial condition at every time step. Without this step, it is likely that no solution will be found.

979-8-3315-8138-1

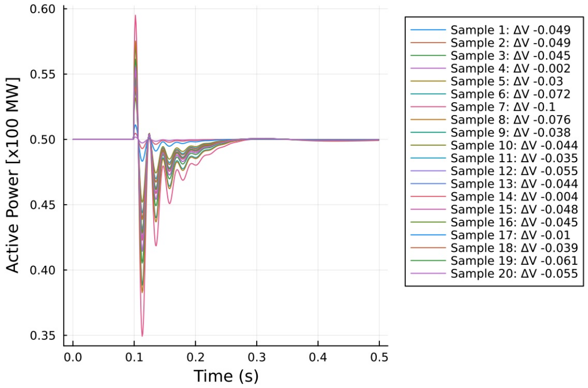

Fig. 8. Active power response for voltage dip with optimal $k_d^* = 93.23$.

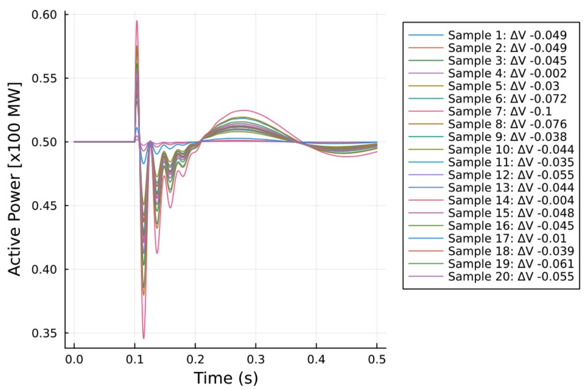

Fig. 9. Active power response for voltage dip with no $k_d = 0$.

- Variables should be bound accordingly to achieve reasonable performance with the solver. Finding good bounds for voltages, currents, and internal states will improve solution times.
- Discretize with the larger step h as possible to reduce the number of variables, depending on the model and perturbation for each case study. Pairing the trajectory optimization approach with a simulation library is crucial for calibration.
- Choose appropriate linear solvers. For example, MUMPS perform significantly worse than HSL. HSL ma57 and ma97 multi-threaded sparse solvers perform well for tuning with the trapezoidal rule.

IV. Conclusions

This paper presents a trajectory optimization approach for tuning parameters in synchronous machines and inverters. We propose various objective functions based on specific case studies to achieve outcomes like effective power tracking and voltage/frequency recovery. Preliminary studies show that our method effectively enhances device compliance automation and when paired with appropriate linear solvers, the interior point method is effective in obtaining a valid solution for the control parameters.

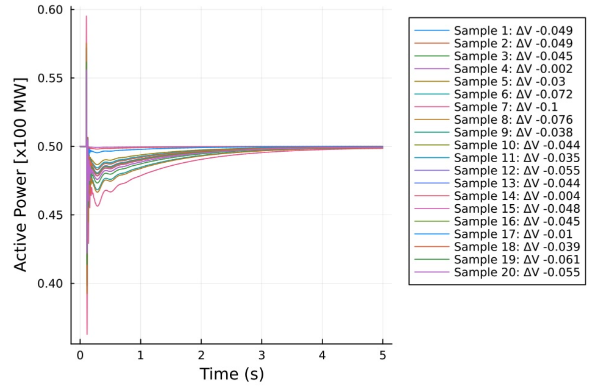

Fig. 10. Active power response for voltage dip with max $k_d = 2000$.

Future work will focus on refining our approach for larger cases and optimizing multiple parameters across various devices. Additionally, exploring GPU techniques for large-scale problems may help improve solution times.

References

[1] F. Milano, F. Dörfler, G. Hug, D. J. Hill, and G. Verbič, "Foundations and challenges of low-inertia systems," in *2018 Power Systems Computation Conference (PSCC)*. IEEE, 2018, pp. 1–25.

[2] S. Johnston, Y. Liu, and C. Yang, "An empirical analysis of the interconnection queue," National Bureau of Economic Research, Tech. Rep., 2023.

[3] H. Sun, Q. Guo, J. Qi, V. Ajjarapu, R. Bravo, J. Chow, Z. Li, R. Moghe, E. Nasr-Azadani, U. Tamrakar *et al.*, "Review of challenges and research opportunities for voltage control in smart grids," *IEEE Transactions on Power Systems*, vol. 34, no. 4, pp. 2790–2801, 2019.

[4] Z. A. Obaid, L. M. Cipcigan, L. Abrahim, and M. T. Muhssin, "Frequency control of future power systems: reviewing and evaluating challenges and new control methods," *Journal of Modern Power Systems and Clean Energy*, vol. 7, no. 1, pp. 9–25, 2019.

[5] A. O'dwyer, *Handbook of PI and PID controller tuning rules*. World Scientific, 2009.

[6] R. P. Borase, D. Maghade, S. Sondkar, and S. Pawar, "A review of pid control, tuning methods and applications," *International Journal of Dynamics and Control*, vol. 9, no. 2, pp. 818–827, 2021.

[7] H. Alrajhi, Y. Al-Harbi, A. Al-Zahrani, S. A. Raza, A. Daraz, and M. Al-Kaabi, "Comprehensive analysis of pi tuning techniques for vsc applications," *Journal of Umm Al-Qura University for Engineering and Architecture*, pp. 1–18, 2025.

[8] M. Kelly, "An introduction to trajectory optimization: How to do your own direct collocation," *SIAM review*, vol. 59, no. 4, pp. 849–904, 2017.

[9] F. Geth, S. Claeys, and G. Deconinck, "Current-voltage formulation of the unbalanced optimal power flow problem," in *2020 8th Workshop on Modeling and Simulation of Cyber-Physical Energy Systems*. IEEE, 2020, pp. 1–6.

[10] J. D. Lara, R. Henriquez-Auba, M. Bossart, D. S. Callaway, and C. Barrows, "PowerSimulationsDynamics.jl–An open source modeling package for modern power systems with inverter-based resources," *arXiv preprint arXiv:2308.02921*, 2023.

[11] A. Wachter, *An interior point algorithm for large-scale nonlinear optimization with applications in process engineering*. Ph.D. Thesis, Carnegie Mellon University, 2002.

[12] F. Milano, *Power system modelling and scripting*. Springer, 2010.

[13] J. Wang, B. Lundstrom, and A. Bernstein, "Design of a non-pll grid-forming inverter for smooth microgrid transition operation," in *2020 IEEE Power & Energy Society General Meeting (PESGM)*. IEEE, 2020, pp. 1–5.

[14] R. Henriquez-Auba, J. D. Lara, C. Roberts, and D. S. Callaway, "Grid forming inverter small signal stability: Examining role of line and voltage dynamics," in *IECON 2020 The 46th Annual Conference of the IEEE Industrial Electronics Society*. IEEE, 2020, pp. 4063–4068.

979-8-3315-8138-1